

ERRATA

Correction to Reviews in Mineralogy & Geochemistry Vol. 53

--- Zircon ---

“Preface” by J. M. Hanchar & P. W. O. Hoskin, p. v-vii

Last full paragraph at the bottom of page vi should read:

The final chapter, by Corfu et al. (Chapter 16), is an atlas of internal textures of zircon. The imaging of internal textures in zircon is essential for directing the acquisition of geochemical data and to the integrity of conclusions reached once data has been collected and interpreted. This chapter, for the first time, brings into one place textural images that represent common and not so common textures reported in the literature, along with brief interpretations of their significance. There is presently no comparable atlas. It is intended that this chapter will become a reference point for future workers to compare and contrast their own images against.

Chapter 1 “Structure and Chemistry of Zircon and Zircon Group Minerals” by R. J. Finch & J. M. Hanchar, p. 1-25

Corrected street address for author Robert J. Finch:

9700 South Cass Avenue

Page 18, line 10 from top of page:

replace “scheelite” with “monazite” such that the line reads:

zircon-type-to-monazite transformations...

Chapter 2 “The Composition of Zircon and Igneous and Metamorphic Petrogenesis” by P. W. O. Hoskin & U. Schaltegger, p. 27-62

Page 29, 9th line from bottom:

Reference to Watson and Hanchar (this volume) should be to Hanchar and Watson (this volume).

Table 2. Rare-earth element and Y composition of standard zircon 91500 (ppm $\pm 1\sigma$)^{*}.

Element	Wiedenbeck ¹	Nesbitt ²	Hoskin ³	Belousova ⁴	Sano ⁵
<i>n</i>	1–6	10	17†	4	5–6**
Y			160 \pm 23	147 \pm 22	
La		0.003	0.04 \pm 0.03		0.01 \pm 0.01
Ce	2.0 \pm 0.1	2.14	2.5 \pm 0.2	2.5 \pm 0.5	2.6 \pm 0.4
Pr		0.01	0.03 \pm 0.02		0.04 \pm 0.02
Nd	0.4	0.25	0.3 \pm 0.1		0.30 \pm 0.06
Sm	0.3	0.50	0.4 \pm 0.1	0.4 \pm 0.2	0.28 \pm 0.08
Eu	0.26 \pm 0.07	0.23	0.22 \pm 0.01	0.4 \pm 0.2	0.19 \pm 0.07
Gd	1.9 \pm 0.1	2.38	2.0 \pm 0.4	2.1 \pm 0.4	1.6 \pm 0.4
Tb		0.83	0.86 \pm 0.06		0.8 \pm 0.2
Dy	8.0 \pm 0.1	10.8	11.03 \pm 0.06	12 \pm 2	12 \pm 3
Ho		4.4	4.8 \pm 0.3	4.9 \pm 0.7	5 \pm 1
Er	20.4 \pm 0.8	24.2	25 \pm 2	26 \pm 4	29 \pm 6
Tm		6.4	6.6 \pm 0.4		8 \pm 2
Yb	57 \pm 17	69.7	65 \pm 2	66 \pm 7	77 \pm 18
Lu	12.4 \pm 0.9	12.6	13 \pm 2	14 \pm 2	17 \pm 4
Σ REE	103+	134	132	128+	154

* A blank entry denotes element not analyzed for or below the limit of detection.

** Uncertainty is given as $\pm 2\sigma$; *n*= the number of analyses contributing to mean REE and Y values.

† Includes SIMS and LA-ICP-MS data.

1. Weidenbeck et al. (1995); 2. Nesbitt et al. (1997); 3. Hoskin (1998); 4. Belousova et al. (2002); 5. Sano et al. (2002).

Table 3. Characteristic ratios of chondrite-normalized zircon REE patterns of Figure 4.[†]

Ratio**	Vaca Muerta zircon 2	Simmern	Lunar/Apollo 14	Phalaborwa carbonatite	Mud Tank carbonatite	Jwaneng kimberlite
Figure 4	a	a	b	c	c	c
<i>n</i>	1	1	1	1	16	4
(Sm/La) _N	1.3	0.4	4.8	164	11.3	38
(Lu/Gd) _N	4.6	169	45	15	9.3	1.4
Ce/Ce*	0.9	1.3	0.6	49	3.7	13
Eu/Eu*	0.2	2.1	0.1	0.4	1.0	1.0

Ratio**	Blind Gabbro	Mawson ig. charnockite	Syros ophiolite	Manilla plagiogranite	BPZP diorite	BPZP aplite
Figure 4	d	d	e	e	f	f
<i>n</i>	8	10	8	7	7	4
(Sm/La) _N	153	236	547	90	119	57
(Lu/Gd) _N	16	19	44	44	27	38
Ce/Ce*	20	79	82	20	39	40
Eu/Eu*	0.2	0.2	0.3	0.9	0.2	0.3

Ratio**	Torihama dacite	Manaslu granite	Chuquicamata W. porphyry	Los Picos diorite	Elie Ness xenolith	Jack Hills zircon
Figure 4	g	h	i	j	k	l
<i>n</i>	6	13	10	9	6	8
(Sm/La) _N	306	33	145	653	165	18
(Lu/Gd) _N	74	—	47	19	17	35
Ce/Ce*	132	—	230	87	31	8.0
Eu/Eu*	0.3	0.3	0.4	0.1	0.9	0.2

† Chondrite normalizing values from McDonough and Sun (1995). Ce_N indicates the element has been normalized; (Sm/La)_N indicates that the elements were normalized prior to division.

n = the number of analyses contributing to mean.

** Anomalies are calculated in this manner; for example Ce/Ce* = Ce_N / (La_N \times Pr_N)^{1/2}.

Chapter 3 “Melt Inclusions in Zircon” by J. B. Thomas, R. J. Bodnar, N. Shimizu and C. A. Chesner, p. 63-87

Page 71, Figure 5, legend:

small boxes following “melt inclusions” should be deleted

Page 73, corrected Table 1:

Table 1. Zircon/melt partition coefficients (D_{REE}) calculated using REE abundances of melt inclusions and coexisting zircon crystals from the Quattoon Igneous Complex and from the Toba rhyolite. [Quottoon Igneous Complex data used by permission of Elsevier Science, from Thomas et al. (2002), *Geochimica et Cosmochimica Acta*, Vol. 66, Table 3, p. 2894]

	D_{La}	D_{Ce}	D_{Nd}	D_{Sm}	D_{Dy}	D_{Er}	D_{Yb}
Quottoon	0.05	2.06	1.58	11.61	72.98	72.39	51.52
	0.04	0.83	0.2	2.7	20.09	29	40.63
	0.07	1.46	0.5	3.56	22.45	29.35	35.88
	0.22	0.99	0.53	4.14	16.79	21.09	21.9
	0.03	1.4	0.77	5.02	19.41	17.89	14.04
	0.02	0.61	0.11	2.49	36.56	58.88	66.1
	0.06	0.93	0.56	4.58	12.37	13.07	13.04
	0.26	1.26	0.81	3.24	51.95	74.99	76.32
	0.02	0.43	0.35	0.75	19.31	52.72	82.29
	0.03	1.1	0.31	11.24	52.31	60.74	35.11
	0.05	0.75	0.16	1.27	26.42	70	96.72
	Median D_M	0.05	0.99	0.5	3.56	22.45	52.72
							40.63
Toba	0.21	0.67	0.41	4.28	11.77	20.29	16.51
	0.04	0.56	0.10	0.99	14.29	20.23	17.70
	*0.01	0.56	0.76	4.71	84.12	220.81	242.70
	0.43	1.35	0.76	5.25	41.83	38.21	32.13
	0.03	0.83	0.12	2.52	29.45	33.56	39.92
	0.03	0.29	0.24	1.32	90.39	19.27	29.74
	*0.01	0.74	0.71	2.22	68.45	187.43	460.31
	0.001	0.55	0.66	3.81	49.48	63.81	86.30
	0.001	0.42	0.10	1.52	22.04	45.75	85.86
	0.02	0.90	0.09	2.61	23.42	29.67	37.44
	0.08	0.17	0.16	0.43	14.48	27.56	36.77
	Median D_M	0.03	0.62	0.25	2.37	26.44	31.61
							37.10

* hourglass shaped inclusions

Page 73, corrected Table 2:

Table 2. Zircon/melt partition coefficients (D_M) calculated for lowest (top row) and highest (bottom row) La, Sm and Yb abundances in the melt inclusions and zircon hosts. [Used by permission of Elsevier Science, from Thomas et al. (2002), *Geochimica et Cosmochimica Acta*, Vol. 66, Table 4, p. 2896]

^a La_{MI}	^b La_{zircon}	D_{La}	^a Sm_{MI}	^b Sm_{zircon}	D_{Sm}	^a Yb_{MI}	^b Yb_{zircon}	D_{Yb}
13.6	0.41	0.03	0.29	3.26	11.24	1.495	144.6	96.72
96.6	2.9	0.03	6.06	30.4	5.02	83.35	1170	14.04

(a) REE abundance in melt inclusion.

(b) REE abundance in zircon.

Page 80, Figure 10, legend:

small boxes following “zircon”, “matrix glass”, “allanite”, and “plagioclase” should be deleted

Page 81, Figure 11, legend

Small boxes following “zircon”, “allanite”, and “plagioclase” should be deleted

**Chapter 4 “Zircon Saturation Thermometry” by J. M. Hanchar & E. B. Watson,
p. 89-112**

Page 92, corrected Table 1:

Table 1. Calculation of *M* and *FM*.

Oxide	N-57 rhyolite (Wark 1991)	Oxide wt % / Eq wt ¹	Cation fraction ²
SiO ₂	69.04	1.149	0.679
TiO ₂	0.38	0.005	0.003
Al ₂ O ₃	13.65	0.268	0.158
FeO	0.63		
Fe ₂ O ₃	1.26		
FeO (t) =	1.76	0.025	0.015
Fe ₂ O ₃ *0.8998+FeO			
MnO	0.07	0.001	0.001
MgO	0.46	0.011	0.007
CaO	1.31	0.023	0.014
Na ₂ O	4.61	0.149	0.088
K ₂ O	2.85	0.061	0.036
P ₂ O ₅	0.04	0.001	0.000
H ₂ O ⁻	0.52		
H ₂ O ⁺	5.07		
CO ₂	0.00		
Total	99.89	1.692	
Zr (ppm) ⁴	299		

³M = (Na+K+(2*Ca))/(Al*Si)
⁴M = 1.41
³FM= (Na+K+(2*Ca+Fe+Mg))/(Al*Si)
⁴FM = 1.69

Notes: Data for bulk sample analysis by X-ray fluorescence spectrometry from Wark (1991).
¹The values in column 3 are calculated from using the wt. % oxide for each major element in column 2 divided by the equivalent wt. for that oxide.
²The values in column 4 are calculated from each value in column 3 divided by the total for column 3.
³The values used in the *M* and *FM* calculations are the cation fractions from column 4.
⁴No error was reported for Zr in Wark (1991).

Page 105, corrected Table 2:

Table 2. Major element comparison between XRF and EMPA for N-57 rhyolite.

Oxide	XRF (bulksample) ¹	EMPA (<i>in situ</i>)
SiO ₂	69.04	69.43
TiO ₂	0.38	0.26
Al ₂ O ₃	13.65	12.74
FeO	0.63	
Fe ₂ O ₃	1.26	
FeO (t) =	1.76	1.02
Fe ₂ O ₃ *0.8998+FeO		
MnO	0.07	“fixed value” ¹
MgO	0.46	0.15
CaO	1.31	0.53
Na ₂ O	4.61	4.76 ²
K ₂ O	2.85	2.94
P ₂ O ₅	0.04	“fixed value”
H ₂ O ⁻	0.52	
H ₂ O ⁺	5.07	“fixed value”
CO ₂	0.00	n/a
Total	99.89	n/a
Zr (ppm) ⁴	299	325 +/- 31 ³

Notes: ¹Only Si, Ti, Al, Fe, Mg, Ca, Na, and K were analyzed with the EMPA. Fixed values for an average rhyolite composition from Best (1982) were used for other elements in ZAF correction.

²Na₂O value in Table 2 corrected to account for Na loss during EMPA analysis (see text).

³Error on EMPA Zr concentration value from 1 σ absolute standard deviation from counting statistics.

Table 3. Temperature and fO_2 estimates for N-57 rhyolite sample.

Sample ¹	Fe-Ti oxide thermometry ²	$\log fO_2$ estimate ²	Two-pyroxene thermometry ²	Bulk sample (XRF) ² M, Zr, and T	<i>In situ</i> glass analysis (EMPA) ³ M, Zr, and T
				1.41	1.35
			@ 0.1 GPa	299 ppm	325 ± 31 ppm
#1	903°C	-10.6	862°C	883°C	
#2	897°C	-10.7	836°C	857°C	
				842°C	855 ± 15 °C

Note: ¹#s 1 and 2 in column 1 refer to two different temperature and fugacity determinations for sample N-57.

²Fe-Ti oxide and pyroxene thermometry (Anderson and Lindsley [1985] and Davidson and Lindsley [1988], respectively), fO_2 estimate, and XRF bulk sample Zr concentration from Wark (1991).

³Error on calculated temperature propagated through from counting statistics uncertainty in Zr determination which is thought to be the largest source of error. Zircon saturation temperatures calculated using Equation 1 in text and data from Tables 1 and 2.

Chapter 5 “Diffusion in Zircon” by D. J. Cherniak & E. B. Watson, p. 113-143

Page 137, Figure 17, missing text at end of caption:

Complete caption should read as follows:

Figure 17. Oxygen diffusion center-retention criteria for spherical zircon cores and rims cooling under wet conditions (Watson and Cherniak, 1997). The schematic diagram in (a) shows a radial profile of $\delta^{18}\text{O}$ (initially a step distribution) which relaxes toward homogeneity with increasing time at high temperature. There is a critical cooling rate— $(dT/dt)_c$, assumed here to be linear—below which the original $\delta^{18}\text{O}$ value at the center of a core or rim will fail to be preserved. If cooling is too slow, $\delta^{18}\text{O}$ will detach from the original core or rim value. The thicker lines show the $\delta^{18}\text{O}$ profile just prior to detachment at the center of the rim (solid line) and of the core (dashed line). The diagram implies a $\delta^{18}\text{O}$ for the surrounding medium equivalent to that of the core but the model results shown in (b) and (c) are independent of the relative $\delta^{18}\text{O}$ values of the core, rim and host medium. (b) and (c) Results of numerical simulation of wet oxygen diffusion to determine the critical minimum cooling rate, $(dT/dt)_c$, for retention of the original $\delta^{18}\text{O}$ value at the center of a spherical zircon crystal or core (b), or rim (c). The dots represent the actual numerical results; the lines are fits to the numerical data given by Equations (7) and (8). See text for additional discussion.

Chapter 9 “Present Trends and the Future of Zircon in Geochronology: Laser Ablation ICPMS” by J. Košler & P. J. Sylvester, p. 243-275

Page 259, corrected Equations (3a), (3b), and (4b):

$$R_{lc} = R_{lm} * \left[\frac{R_{2c}}{R_{2m}} \right]^{\left(\frac{\Delta M_1}{\Delta M_2} \right)} \quad (3a)$$

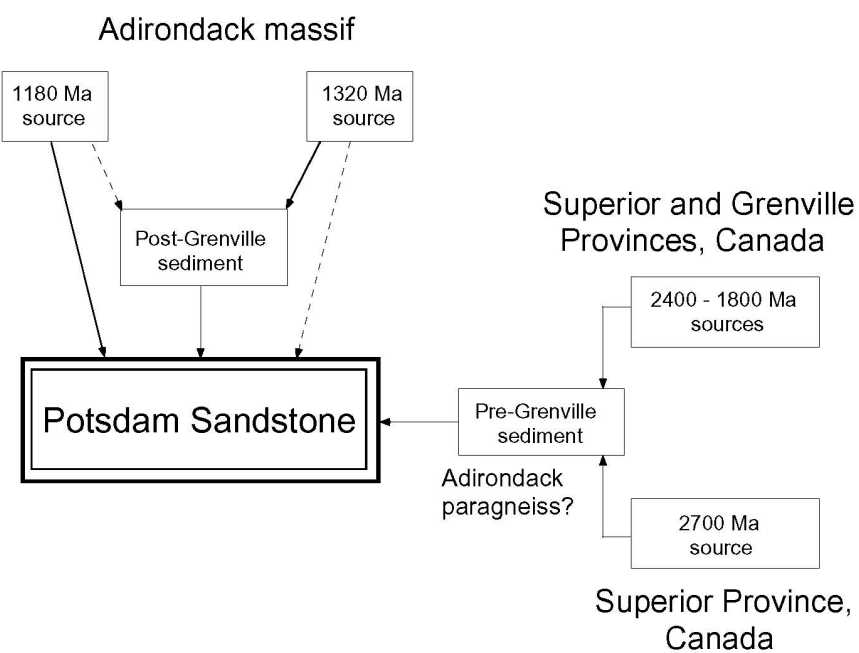
$$\left(\frac{^{207}Pb}{^{235}U} \right)_c = \left(\frac{^{207}Pb}{^{235}U} \right)_m * \left[\frac{\left(^{205}Tl / ^{237}Np \right)_c}{\left(^{205}Tl / ^{237}Np \right)_m} \right]^{\left(\frac{M_{235}-M_{207}}{M_{237}-M_{205}} \right)} \quad (3b)$$

$$\left(\frac{^{207}Pb}{^{235}U} \right)_c = \left(\frac{^{207}Pb}{^{235}U} \right)_m * \left[\frac{\left(^{205}Tl / ^{237}Np \right)_c}{\left(^{205}Tl / ^{237}Np \right)_m} \right]^{\left[\frac{\ln(M_{235}-M_{207})}{\ln(M_{237}-M_{205})} \right]} \quad (4b)$$

Chapter 10 “Detrital Zircon Analysis of the Sedimentary Record” by C. M. Fedo, K. N. Sircombe & R. H. Rainbird, p. 277-303

Page 293, Figure 4 (missing left edge of figure):

corrected figure –



Chapter 12 “Lu-Hf and Sm-Nd Isotope Systems in Zircon” by P. D. Kinny & R. Maas, p. 327-341

Page 328, Figure 1, caption:

Corrected caption should read:

Figure 1. Schematic Hf isotope evolution diagram, modified after Patchett et al. (1981), showing how an episode of partial melting in Earth’s mantle at time t_1 results in divergent Hf isotope evolution paths for the newly generated crust (low Lu/Hf) and the residual mantle (high Lu/Hf). Having extremely low Lu/Hf, any zircons formed within that crust will preserve its initial $^{176}\text{Hf}/^{177}\text{Hf}$ ratio, and hence over time diverge in composition from the remainder of the host rock. At time t_2 a variety of possible sources may contribute to newly formed crust. If wholly derived from depleted mantle the initial ϵ_{Hf} will be positive, however mixing with an undepleted or enriched source, for example by crustal contamination, may result in low positive, zero, or negative ϵ_{Hf} at the time of crystallization depending on the balance of components. Any inherited zircon cores at t_2 would be expected to have lower ϵ_{Hf} than the newly-crystallized host rock.

Page 329, corrected Table 1:

Table 1. Bulk unfractionated silicate Earth reference parameters.

$(^{176}\text{Hf}/^{177}\text{Hf})_{\text{today}}$	$(^{176}\text{Lu}/^{177}\text{Hf})_{\text{today}}$	$(^{176}\text{Hf}/^{177}\text{Hf})_{\text{init}}$	Parameters for initial Hf	Reference
0.28286 ± 9	0.0334	0.27978 ± 9	t_0 4.55 Ga; λ_{Lu} 1.94×10^{-11}	1
0.282772 ± 29	0.0332 ± 2	0.279742 ± 29	t_0 4.56 Ga; λ_{Lu} 1.93×10^{-11}	2

1. Tatsumoto et al. 1981. 2. Blichert-Toft and Albarède 1997.

Chapter 13 “Oxygen Isotopes in Zircon” by J. W. Valley, p. 343-385

Page 345, Table 1:

Corrected row 1 (missing subscript and superscripts now included):

Standard	$\delta^{18}\text{O}$ ‰ SMOW	$\pm 1\text{SD}$	N	age Ma	U ppm	HfO_2 wt%	Refs.	Comments
----------	---------------------------------	------------------	---	-----------	----------	-----------------------	-------	----------

Page 348, Table 2:

Equation (1) in bottom row of table should read:

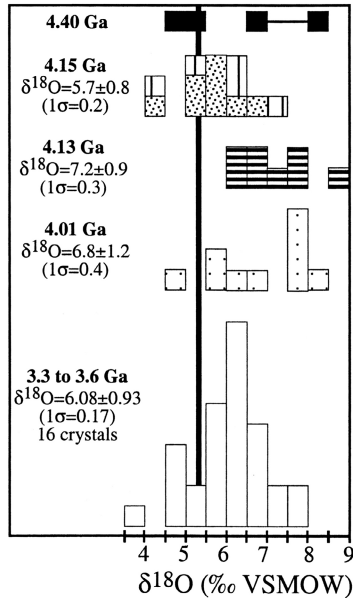
Eqn 1: $1000 \ln(\alpha_{\text{A-B}}) = A_{\text{A-B}}(10^6/T^2)$, (T in K). Values should be extrapolated below ~600°C

Page 357, Figure 13, caption:

The six occurrences of “d¹⁸O” in this figure caption should be replaced with “δ¹⁸O” (found in lines 1, 3, 5, 10, 14 and 20 of caption)

Page 359, Figure 15:

Correct figure is:



Correct figure and figure caption are:

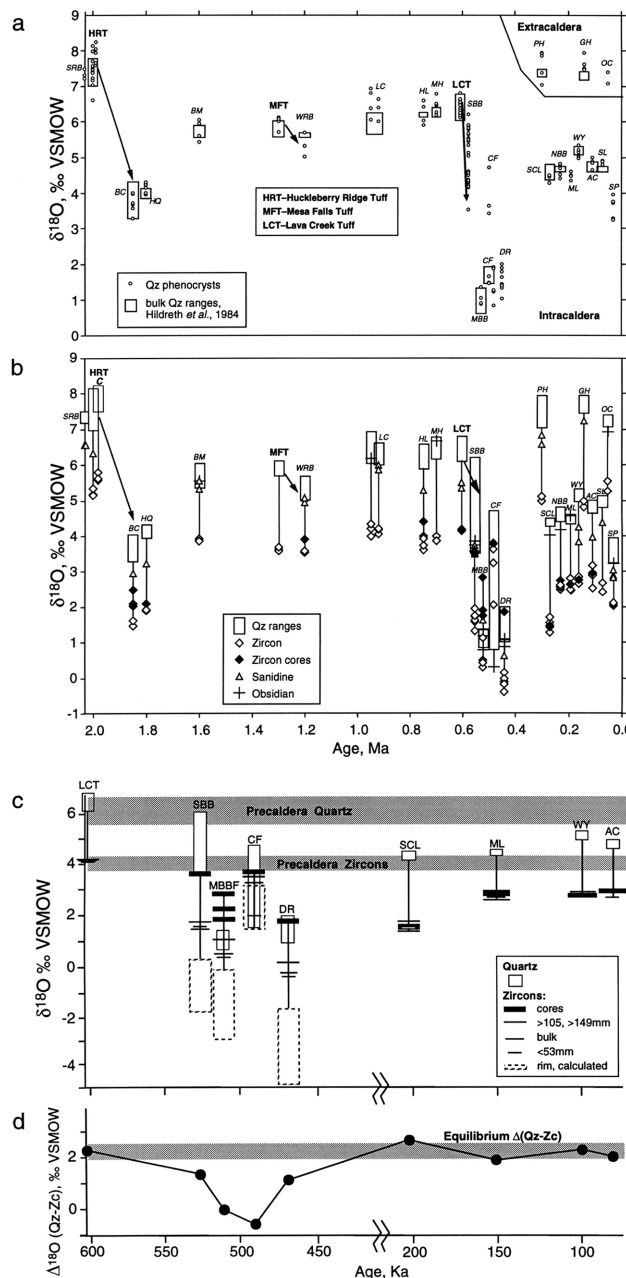


Figure 23. Evolution of $\delta^{18}\text{O}$ in Yellowstone magmas. Caldera-forming eruptions are Huckleberry Ridge Tuff (HRT), Mesa Falls Tuff (MFT), and Lava Creek Tuff (LCT). (a) Individual quartz phenocrysts and bulk quartz. (b) Zircon, sanidine, and obsidian. Air-abraded zircon cores are filled diamonds. (c) Post LCT intra-caldera lava flows. The range of individual quartz phenocrysts are shown in boxes. Zircons are plotted by crystal size. (d) $\Delta^{18}\text{O}(\text{Qt-Zc})$ for LCT and post-LCT lavas. The equilibrium value of $\Delta(\text{Qt-Zc})$ is 1.9–2.3‰ at 800–900°C. Note that only low $\delta^{18}\text{O}$ rhyolites have quartz and zircon that are not equilibrated (from Bindeman and Valley 2000a, 2001).

Page 371, Figure 29, caption:

In line 1 of the caption, “ $d^{18}O(Zc)$ ” should be “ $\delta^{18}O(Zc)$ ”.

Page 383, King et al. (2003b) reference – remove (in review) from citation

Page 384, Peck et al. (2003a) reference – remove (in press) from citation

Page 385, Valley et al. (2003) reference – remove (in press) from citation

Chapter 14 “Radiation Effects in Zircon” by R. C. Ewing, A. Meldrum, LuMin Wang, W. J. Weber and L. R. Corrales, p. 387-425

All even pages, running header:

Should read: Ewing, Meldrum, Wang, Weber, Corrales:

Page 405, Figure 9, caption:

Caption should read:

Figure 9. Crystalline-to-amorphous transition plotted as functions of equivalent uranium content and age. The lower curve represents the onset of observable damage as measured by electron diffraction, and the upper curve is for “complete” amorphization, at a temperature of 100°C. The open squares represent natural “crystalline” zircon from a variety of locations whose age and equivalent uranium content were measured or calculated. The filled triangles are for “amorphous” natural zircon from different localities. The curves delineate the crystalline-amorphous boundary fairly well, despite the different thermal histories and geologic environments of the different specimens. At higher ambient temperatures, the transitions would be shifted to higher uranium content. [Modified after Meldrum et al. (1999a).]

Page 414, Figure 12, caption:

Caption should read:

Figure 12. Calculated number of vacancies produced along the path of 4.6 MeV alpha particles in zircon, along with the distribution of alpha particle ranges, using the BCA code SRIM.

Chapter 15 “Spectroscopic Methods Applied to Zircon” by L. Nasdala, M. Zhang, U. Kempe, G. Panczer, M. Gaft, M. Andrut, & M. Plötze, p. 427-467

Page 444, 3rd line from bottom:

“observed with $E \parallel c$ ” should read “observed with $E \perp c$ ”